 doi:10.20944/preprints202207.0461.v1

Article

A Dependable Digital System Model for Malaria Monitoring

Carine Pierrette Mukamakuza [1], Emmanuel Tuyishimire [2], Aimable Mbituyumuremyi[3], Timothy X Brown[1], Didier Iradukunda [1], Ofentse Phuti[1], Happiness Rose Mary[1]

[1] College of Engineering, Carnegie Mellon University Africa, Kigali, Rwanda.
[2] Department of Computer Science, Institut d'Enseignement Supeŕieur, Ruhengeri, Rwanda.
[3] Rwanda Biomedical Centre.
* Correspondence: cmukamak@andrew.cmu.edu; temmanuel@uwc.ac.za

Abstract: Malaria is a long-standing disease and one of the top life-threatening diseases, yet its treatment has not changed, while the world has already embraced the Fourth Industrial Revolution (4IR). A wave of research on digitizing monitoring mechanisms of such a deadly disease has surfaced. Automated malaria screening is one of the detection processes which are gaining popularity in the research domain. However, the process needs to be coupled with other processes aiming a nationally or regionally contextualised malaria monitoring system. This paper proposes a digital malaria monitoring system in the context of an African country or region. One advantage of such a digital system is that is enables a novel disease spread forecasting model based on the dynamics of different malaria types. The architecture of the diagnosis system is described, and the disease spread model is mathematically modelled in terms of a SPITR (Susceptible- Protected- Infected-Treated- Recovered) epidemic model which is further analysed. The forecasting model is expressed and analysed whereas experiments are conducted using a Monte Carlo simulation method. The design of the monitoring system has inspired how predictions can be made in the complex cases such as mixed infections. Results show that reinforcing the model parameter makes a significant improvement on the disease prediction.

Keywords: Malaria; digital; epidemic; mixed infections; reinforcement.

1. Introduction

Technology has been widely used to mitigate many issues caused by the COVID-19 pandemic while contributing to the pandemic control and treatment. This inspires us to revisit how digital technology may be used with existing diseases for more efficient management. This paper revisits a malaria monitoring and treatment and then look at hte role of digital technology in more accurately forecasting spread of the disease.

Malaria is a long-standing disease caused by a plasmodium parasite transmitted through the biting of an infected female Anopheles mosquito. The severity of such a disease depends on the involved types of transmitted parasites, which may be Plasmodium falciparum, Plasmodium vivax, Plasmodium ovale curtisi, Plasmodium ovale wallikeri, Plasmodium malariae and the very rare Plasmodium knowlesi, as reported in [1].

Malaria is one of the most life-threatening diseases which is, however, curable. In 2021, 241 millions cases have been recorded and a total of 627 thousand malaria-deaths have been estimated. Africa has been the most affected region having 90% of the total global cases and 90% of the malaria deaths have been found in Africa. Of these death, 77% were children under 5 years old [2]. On the other hand, since 2009, many African countries have required that all malaria cases need to be confirmed through parasitology tests, using light microscopy. However, microscopy is a time-consuming process whose efficacy varies based on many factors including the viral load, the course of infection, and the skill of the technician. While skilled technicians can detect malaria with a Plasmodium density of 30 parasites per micro litre of smeared blood, novice ones may require up to 100 parasites per micro litre to be present [3]. With such a wide variance, it is unsurprising that a meta-analysis on the comparative effectiveness of different malaria parasitology tests found that light microscopy missed up to 50% of cases (diagnosed via real-time Polymerase Chain Reaction Tests i.e. PCR) [4].

Citation: Lastname, F.; Lastname, F.; Lastname, F. Title. *Preprints* **2021**, *1*, 0. https://doi.org/

Received:
Accepted:
Published:

 doi:10.20944/preprints202207.0461.v1

Despite this, using microscopy on stained blood smears remains the best choice for malaria diagnosis in resource-limited environments for several reasons:

- It is less costly than PCR and rapid diagnostic tests (RDTs).
- It can be more accurate than RDTs.
- It can provide an actual count of the number of Plasmodium species in a blood smear, potentially indicating the degree of severity of the illness and allowing more accurate treatment from the onset.
- It can identify the different species of Plasmodium, unlike RDTs which only confirm the presence or absence of Plasmodium.
- Identifying the species of Plasmodium allows more precise treatment and modeling of malaria infections.

In recent years, researchers have focused on developing automated malaria screening tools to enable the provision of time-sensitive and high-accuracy diagnostics. Usually, artificial intelligence is used to detect, and sometimes quantify, plasmodium in Giemsa-stained thick and thin Giemsa-stained blood smear images. In [5], the authors developed an Android application which is capable of capturing high-resolution images via the smartphone's camera, detecting plasmodium Falciparum, visualizing and locally storing results for future upload. The smartphone itself is mounted on the light microscope. In a test with 50 patients, they achieved a sensitivity of 94.7% and specificity of 97.2% for thin smears and 79.33% and 74% for thick smears.

The application constitutes a promising diagnosis model, but further field trials are needed to assess its efficacy with a larger set of test data and under differing contexts, as preparation of slides can vary from place to place and from person to person.

There are several benefits of using automated malaria screeners:

- First, the screeners can be used to support training of technicians in screening for Plasmodium. Trainee technicians can use the tool to verify that their manual counts and draw attention to Plasmodium that may have been erroneously counted or missed.
- Second, the screeners can be deployed in the field for limited time periods to monitor and evaluate how well field technicians in different locations are performing in malaria diagnosis. This can ensure corrective measures such as retraining are quickly provided to those who need them.
- Finally, the screeners can be deployed in areas where technicians may be scarce. In these settings, any health worker can take the image of the blood smear and get an automated result of the potential severity of the malaria infection (based on the Plasmodium count) and of the type of Plasmodium species causing infection, allowing better prescriptions to be provided.

Preprints (www.preprints.org) | NOT PEER-REVIEWED | Posted: 29 July 2022 doi:10.20944/preprints202207.0461.v1

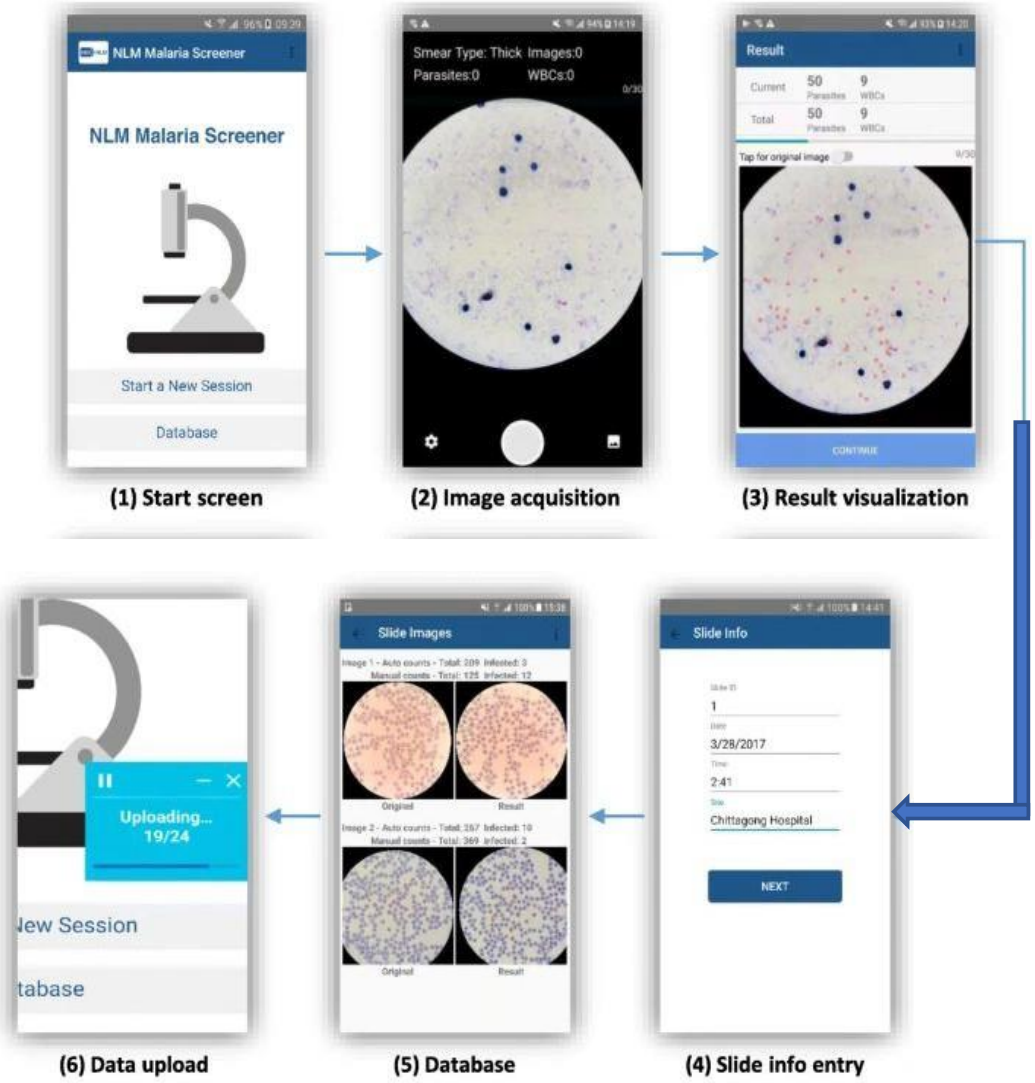

Figure 1. Malaria Screening Tool by Yu et al (2020)[5]

Furthermore, malaria automated screeners can be complemented with storage, communication and computation capabilities to aggregate slide sample data and make more accurate spread predictions on malaria cases.

The spread of a disease has been a subject of mathematical modelling. Many thanks go to the authors in [6] who introduced the, so-called, SIR model for a disease spread in general which partitions the population into three compartments namely Susceptible, Infected and Recovered. The model is a system of ordinary differential equations where constant coefficients have been assumed. This model has inspired other various spread models with various applications, including, wireless technologies [7,8], Economics [9], etc., but a great emphasis has been put in disease modelling.

One such model has been developed for malaria [10]. Here, people have been grouped in terms of Susceptible (S), Exposed(E), Infected(I) and Recovered (R). Susceptible people are defined as those who host the disease, Exposed are people who are infected by the pathogen but cannot pass on the infection to others, Infected people are those who may give rise to more infected people through interaction and finally, the recovered people are those who have recovered from the disease. In different implementations of this model, some models have assumed constants parameters while others have estimated the parameters based on existing data. However, the assumption that some people could, directly, pass on malaria to each other has been incorrectly made as malaria is not contagious [1].

 doi:10.20944/preprints202207.0461.v1

Furthermore, although data could be used to validate the models [11], reinforcement and prediction of the parameters could have been used to ensure more efficient forecasting models. Here, the effect of external conditions such as seasonality patterns [12,13], temperature and rainfall [14], socio-economic factors [15–20], population immunity [21], etc. [11,22–27], could be analysed in a number of models, but it has been mentioned in [10] that, no model could successfully combine all the conditions. This shows that efficient malaria forecasting would depend on local settings such as national or regional with specific determinants, where coefficients would need to be frequently updated.

On the other hand, several models for collecting malaria data have surfaced. It is nowadays possible to capture the microscope images, analyse and use them to digitally test malaria [4]. This approach can benefit from existing data collection and transport models such as [28–30] to be aggregated on a national or regional level, where they can further be processed for a prediction, reinforcement and visualisation.

This paper first proposes a central system for malaria data collection, delivery, storing, preprocessing and visualisation. Various operations on the system, aiming the data analysis, update and model reinforcement, are explained. Building on such a modern data management system, this paper further proposes a predictive model which considers a mixture of malaria variants. The model is complimented with a well defined reinforcement scheme for precision purpose. Lastly, the proposed model is analysed and related experiments are conducted in a multi-regional space.

The rest of this paper is organise as follows. Section 2 covers the architecture of the proposed digital system, in Section 3 the proposed epidemic model is detailed, the system performance is studied in Section 4 and Section 5 concludes the paper, while suggesting future works.

2. Proposed architecture

In this section, we propose the architecture of a data management system aiming the efficient data collection and process for improving the aspects of malaria forecasting. Here, we are inspired by a Cyber-Physical system which is dependable for Internet of Things (IoT) applications, as proposed in [31]. The system consists of an IoT system which enables data collection for the system forecasting purpose.

On the other hand, the World Health Organisation (WHO) has illustrated a digital system model for malaria surveillance in [32]. Here, a data and information flow systems has been briefly described for national decision making purpose. However, the mechanisms and technology to enable the system, in the African context would complement the proposed work.

Preprints (www.preprints.org) | NOT PEER-REVIEWED | Posted: 29 July 2022 doi:10.20944/preprints202207.0461.v1

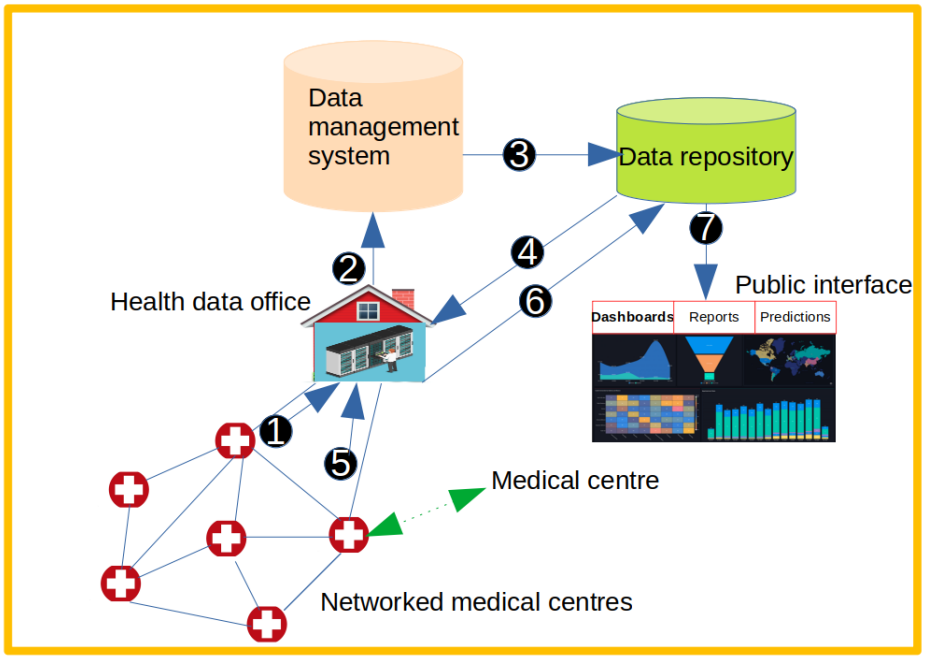

Figure 2. Proposed model

This section describes the system as an object of five main components (instances) and 7 main operations (methods). we discuss them as follows.

2.1. The system components

The system components include the networked medical centres, health data office, a data management system, a repository and a public interface for data reporting and visualisation.

2.1.1. Networked medical centres

It is well known that Africa is the least connected continent [33]. Consequently, the communication network of all medical centres is not necessarily efficient for digital data routing. This is why medical centres may be connected as a network $G(N, L, s)$, where N is the set of all medical centres, L is the set of all possible inter-centres communication links. Here, the communication links may be electronic, terrestrial roads (which could be used by vehicles to move data from one centre to the other) and the aerial possible roads which might be used by the Unmanned Aerial Vehicles (UAVs). Finally, s is the health data office where digital data from medical centres are delivered for further processes. The network may be organised for efficient performance. For instance, medical centres may be clustered based on the optimal cost of communication [29,30,34].

2.1.2. Health data office

The health data office consist of computational and communication tools operated by Data Scientists. As proposed in [35,36], the performance and reliability are two main issues to consider while designing such office.

2.1.3. Data management system

This is the database system where all delivered data are gathered. This system is designed as a Cloud storage and computing, where various Quantity of Services are ensured. These include, resource allocation, data modelling, data availability, data security, etc. [37].

 doi:10.20944/preprints202207.0461.v1

2.1.4. Data Repository

Gathered data are cleaned and classified/categorised in a cloud native repository [38]. Part of such clean data may be visualised to the authenticated public and another part to the Data Scientists for further processes and recommendations.

2.1.5. Public interface

The public interface is where all public reports, dashboards, maps and statistics are visualised for the authenticated public. The Graphic User Interfaces (GUIs) [39,40] are to be explored for more efficient and user friendly interfaces.

2.2. The system operations

2.2.1. Operation 1: Data collection and delivery

Digital datasets are captured from medical centres. These could be the patients' details together with their digitised blood samples (images for example). Based on communication constraints, data may be locally captured and analysed to assist patients. Available means, such as electronic [41,42], aerial vehicles (UAVs [28,43–47] or terrestrial vehicles, may be used to deliver the data to the health data centres for further processes.

2.2.2. Operation 2: Data aggregation

Captured datasets are stored in a database [48], where they may be accessed by Data Scientists for further processes and analysis.

2.2.3. Operation 3: Data classification

Categorisation methods such as deep learning methods [49] may be used to classify collected images (data). Two classifications are important here: positive or negative cases and identifying which type of the involved parasite(s) for each positive case. Cases may be clustered in terms of age, demography etc., to inform various policy makers [50].

2.2.4. Operation 4: Queries responding

Test results, preliminary neural networks and clusters are communicated back to the health data center and forwarded them to the medical centre for local malaria diagnosis. Filtering capabilities, such as the model proposed in [51], may be made available to ease queries responses.

2.2.5. Operation 5: Treatment reporting

For each positive case, treatment details may be communicated to the health data center for reporting purpose.

2.2.6. Operation 6: Repository update

This consists of reinforcing neural networks [52,53] and clustering [53] models while aggregating the treatment related data. Furthermore, disease related model may be reinforced by updating their parameters, based on the new records. For further disease analysis, it is important to record treatment details in the data repository.

2.2.7. Operation 7: launching public information and services

Now that all the malaria datasets are well organised in the repository, they may be visualised, on a well designed GUI, for public or authenticated users for future use. Furthermore, recorded data may be used for further analysis such as forecasting.

3. Disease modelling and prediction

Using the data processing model described in Section 2, available data may be used for forecasting purpose. In this section, a mathematical model is proposed and explained for malaria forecasting purpose. We have been inspired by the SPITR (Susceptiple, Protected, Infected, Treated and Recovered) model proposed in [54], which is an epidemic model

 doi:10.20944/preprints202207.0461.v1

for malaria. In this paper, the model has been extended by considering various types of malaria determined by different mixture of parasites species. Emphasis has been limited to the data which may be made available by the proposed system and hence, the issues of natural death, population motions and dynamics have not been considered.

3.1. Disease compartments

The proposed spread model assumes 5 compartments, namely, Susceptible, Infected, Recovered, Protected, Treated. In this section, we describe the compartments and their interaction in the case of mixed infection.

The number of species of malaria parasites varies with countries, and changes with time. This is why we assume, without loss of generality, that the number of species in a country is a constant denoted by N. A malaria type is determined by the kind of one or many parasite species present in someone's blood.

Proposition 1. *The number of malaria types. Given that the number of malaria parasites in a region is $N \geq 0$, if any subset of the parasites can live in an individual's blood, the number of malaria types in that region is*

$$n = 2^N - 1 \tag{1}$$

For example, in a region where only two parasite species exist, $n = 2^2 - 1 = 3$. These three types correspond to the following scenarios.

1. Scenario 1: it consists of the malaria type where only the first parasite is observed.
2. Scenario 2: it consists of the malaria type where both the first and the second parasite are observed.
3. Scenario 3: it consists of the malaria type where only the second parasite is observed.

It is important to note that Proposition 1 is justified by the fact that The number of subsets of N elements (species in our case) is 2^N. So, removing the empty set (absence of any parasite species) leaves $n = 2^N - 1$.

It is important to note that in the case where two or more parasites can not live together to make a mixed infection, the number of malaria type in the corresponding region, as suggest in Proposition 1 may be restricted to such constraint.

Based on the types of malaria, we define the spread compartments as follows.

1. Susceptible people ($\mathcal{S}$): The set $\mathcal{S}$ consists of people who are exposed to the disease. The cardinality of the set is defined by a column matrix S whose j^{th} entries corresponds to the number of susceptible humans of the j^{th} type of the disease.

$$S = \{s_i\}_{j=1}^{n}$$

Where n is the number of disease types.

2. Protected ($\mathcal{P}$): Some of susceptible people may consider to take some protective measures such as IRS and or ITN to be immune for a period of time and once such a period elapses, some of these people may be susceptible again. The cardinality for such a set is expressed by the following column matrix.

$$P = \{p_i\}_{j=1}^{n}$$

3. Infected people ($\mathcal{I}$): it is the set of people who have been contaminated. These are the people who have been either susceptible or protected and their protection period elapsed.

$$I = \{i_j\}_{j=1}^{n}$$

4. Treated people ($\mathcal{T}$): this is the set of people who have been contaminated and are consuming medicines. It is here assumed that such people cannot be exposed to the

Preprints (www.preprints.org) | NOT PEER-REVIEWED | Posted: 29 July 2022 doi:10.20944/preprints202207.0461.v1

same disease for which they are being taking medicines. After treatment, people may, immediately, take protection measures for them to remain protected for some time. The number of Treated people may be expressed in terms of the following column vector.

$$T = \{t_j\}_{i=1}^{n}$$

It is important to note that malaria treatment is not always type oriented. That is, various malaria variants my be treated at the same time even if one variant has been detected.

5. Recovered people ($\mathcal{R}$): it is the set of people who have been successfully cured because of the medical treatment or traditional healing. Here, it is important to mention that in deep villages, some people may use some plants and successfully cure malaria. In this case we assume that all malaria variants have been cured. Such treatment may be recorded using local health advisors, who are nationally recognised ("Abajyanama b'ubuzima" for example, in the case of Rwanda). These people may become protected for a small period, and later, they may consider taking protection measures. Furthermore, such people may become exposed to the disease again. The cardinality of Recovered people is expressed by the following column matrix.

$$R = \{r_j\}_{j=1}^{n}$$

Note that people may die from any compartment due to various reasons other than malaria. Furthermore, Infected and Treated people may die due to malaria. Infected people die because of limited access to medical attention, and Treated people die because of poor treatment timing or uncontrolled patient metabolisms. The proposed system in this paper does not cover death as it is hard to quantify malaria-dead people, in a developing world. Here, death causes are investigated mostly when they are court cases involved, and this makes it difficult to record malaria-dead people. We, therefore, reserve this important compartment for future research.

3.2. Spread modelling

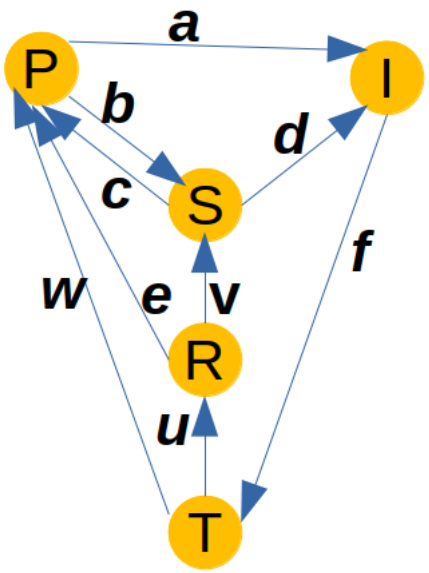

Figure 3. Spread model.

Figure 3 shows the spread rates, expressed as compartment migration rates. For example, the rate of migrating from Susceptible to Infected is denoted by d and from Treated to Protected, the rate is denoted by w.

Preprints (www.preprints.org) | NOT PEER-REVIEWED | Posted: 29 July 2022 doi:10.20944/preprints202207.0461.v1

Taking account to all cases discussed in Section 3, we obtain the following difference equation.

$$\begin{cases} S'_j = -d_j S_j - c_j S_j + b_j P_j + v_j R_j \\ P'_j = c_j S_j - a_j P_j - b_j P_j + w_j T_j + e_j R_j \\ I'_j = d_j S_j + a_j P_j - f_j I_j \\ T'_j = -u_j T_j - w_j T_j + f_j I_j \\ R'_j = u_j T_j - v_i R_i - e_i R_i \end{cases} \tag{2}$$

Note that S_j, P_j, I_j, T_j and R_i are functions of time t for each variant j. The negative rates in the model represent a decrease, whereas the positive ones represent an increase.

Considering the Hadamard product (element wise multiplication of matrices) Equation 2 becomes

$$\begin{cases} S' = \mathbf{b}P + \mathbf{v}R - \mathbf{d}S - \mathbf{c}S \\ P' = -\mathbf{a}P - \mathbf{b}P + \mathbf{c}S + \mathbf{e}R + \mathbf{w}T \\ I'_j = \mathbf{a}P + \mathbf{d}S - \mathbf{f}I \\ T'_j = \mathbf{f}I - \mathbf{u}T - \mathbf{w}T \\ R' = \mathbf{u}T - \mathbf{v}R - \mathbf{e}R, \end{cases} \tag{3}$$

where the parameters **a**, **b**, **c**, **d**, **e**, **f**, **u**, **v** and **w** are vectors of parameters whose entries correspond to the variants of the disease.

3.3. Stability analysis

We study the stability of the system represented in Equation 2. This is done by first computing the Disease-Free Equilibrium (DFE) based on which the basic reproduction number R_0 is computed.

3.3.1. Disease-Free Equilibrium (DFE)

Equation 2 may be written in the following simplified forms.

$$\begin{cases} S'_j = (-d_j - c_j) S_j + b_j P_j + v_j R_j \\ P'_j = c_j S_j + (a_j + b_j) P_j + w_j T_j + e_j R_j \\ I'_j = d_j S_j + a_j P_j - f_j I_j \\ T'_j = (-u_j + f_j) I_j - w_j T_j \\ R'_j = u_j T_j - (v_i + e_i) R_i \end{cases} \tag{4}$$

Alternatively, the equation may be written in a matrix form.

$$D' = MD \tag{5}$$

$$M = \begin{pmatrix} (-d_j - c_j) & b_j & 0 & 0 & v_j \\ c_j & (a_j + b_j) & 0 & w_j & e_j \\ d_j & a_j & -f_j & 0 & 0 \\ 0 & 0 & (-u_j + f_j) & -w_j & 0 \\ 0 & 0 & 0 & u_j & -(v_i + e_i) \end{pmatrix}, \text{ and } D = \begin{pmatrix} S_j \\ P_j \\ I_j \\ T_j \\ R_j \end{pmatrix}$$

The DFE points are solution to Equation 6.

$$MD = 0, \;\; I_j = 0 \tag{6}$$

The determinant of M is clearly not trivially zero. This is why there may be the following two cases.

Case1:

Preprints (www.preprints.org) | NOT PEER-REVIEWED | Posted: 29 July 2022 doi:10.20944/preprints202207.0461.v1

If $detM \neq 0$, then $(S_j, P_j, I_j, T_j, R_j) = (0,0,0,0,0)$ is the unique solution of Equation 6. This is the case where no human in any compartment exists in the corresponding region and hence no human exists in the region at all, as we assumed that any existing human have to belong in one of the disease compartments.

Case2:

If $detM = 0$, then the system of equations 6 has infinitely many solutions, and thus the system will have infinite number of DFE points whose form is $E = (S_j^*, P_j^*, 0, T_j^*, R_j^*)$, where the other components may not all be zero.

3.4. Stability at DFE

We study stability using the basic reproduction number R_0. We calculate R_0 using the next-generation matrix approach as described in [55].

From Equation 4, we deduce the transmission ($\mathcal{F}_j$) and transition ($\mathcal{V}_j$) subsystems, respectively as follows.

$$\mathcal{F}_j(S_j^*, P_j^*, 0, T_j^*, R_j^*) = \begin{cases} 0 \\ 0 \\ d_j S_j^* + a_j P_j^* \\ 0 \\ 0 \end{cases} \tag{7}$$

$$\mathcal{V}_j(S_j^*, P_j^*, 0, T_j^*, R_j^*) = \begin{cases} (-d_j - c_j)S_j^* + b_j P_j^* + v_j R_j^* \\ c_j S_j^* + (a_j + b_j)P_j^* + w_j T_j^* + e_j R_j^* \\ -f_j I_j^* \\ (-u_j + f_j)I_j^*, -w_j T_j^* \\ u_j T_j^* - (v_i + e_i)R_i^* \end{cases} \tag{8}$$

The next-generation matrix is $K = FV^{-1}$, where F and V are the Jacobian matrices of $\mathcal{F}$ and $\mathcal{V}$ respectively, evaluated at the DFE.

Case1:

If $detM \neq 0$, the DFE is $E_0 = (S_j^*, P_j^*, 0, T_j^*, R_j^*) = (0,0,0,0,0)$, and the Jacobian of $\mathcal{F}$ evaluated at E_0 is

$F_{ij}(E_0) = \frac{\partial \mathcal{F}_i}{\partial e_j}(E_0)$ and it is the zero matrix.

Consequently, the matrix $K = FV^{-1}$ is the zero matrix. The eigenvalues of the matrix K are all zero and hence the basic reproductive number is $R_0 = 0$. Since $R_0 < 1$, the DFE E_0 is globally stable. This means that the region with no human, will never witness new infections. Instead of this observation only showing the stability of the system, it rather shows the accuracy of the system.

Case2:

If $detM = 0$, then the system of equations (6) has more than one solutions, and thus the system will have more than one DFE points denoted by $(S_j^*, P_j^*, 0, T_j^*, R_j^*)$.

$$F = \begin{pmatrix} 0 & 0 & 0 & 0 & 0 \\ 0 & 0 & 0 & 0 & 0 \\ d_j & a_j & 0 & 0 & 0 \\ 0 & 0 & 0 & 0 & 0 \\ 0 & 0 & 0 & 0 & 0 \end{pmatrix} \tag{9}$$

Preprints (www.preprints.org) | NOT PEER-REVIEWED | Posted: 29 July 2022 doi:10.20944/preprints202207.0461.v1

$$V = \begin{pmatrix} (-d_j - c_j) & b_j & 0 & 0 & v_j \\ c_j & (a_j + b_j) & 0 & w_j & e_j \\ 0 & 0 & -f_j & 0 & 0 \\ 0 & 0 & (-u_j + f_j) & -w_j & 0 \\ 0 & 0 & 0 & u_j & -(v_i + e_i) \end{pmatrix} \tag{10}$$

Using Sage math [56], the basic reproduction number for the malaria type j, denoted by R_0^j is calculated as follows.

$$R_0^j = Trace(F_j V_j^{-1}) =$$

$$d_j \left(\frac{(f_j - u_j)u_j \left(\frac{b_j \left(e_j + \frac{c_j v_j}{c_j + d_j} \right)}{\left(a_j + b_j + \frac{b_j c_j}{c_j + d_j} \right)(c_j + d_j)} - \frac{v_j}{c_j + d_j} \right)}{(e_j + v_j) f_j w_j} + \frac{b_j (f_j - u_j)}{\left(a_j + b_j + \frac{b_j c_j}{c_j + d_j} \right)(c_j + d_j) f_j} \right)$$

$$+ \quad a_j \left(\frac{f_j - u_j}{\left(a_j + b_j + \frac{b_j c_j}{c_j + d_j} \right) f_j} + \frac{\left(e_j + \frac{c_j v_j}{c_j + d_j} \right)(f_j - u_j)u_j}{\left(a_j + b_j + \frac{b_j c_j}{c_j + d_j} \right)(e_j + v_j) f_j w_j} \right).$$

So, the basic reproduction number R_0 for the corresponding region is calculated as follows.

$$R_0 = \sum_{j=1}^{2^N - 1} R_0^j$$

If $R_0 > 1$, the new infections are expected and if $R_0 < 1$, no new infection would be expected.

Note that R_0, algebraically, only depends on the coefficients, which are the transmission rates. However, these rates are implicitly related to the DFE and time. To clarify this, we discuss the way these rates may be periodically reinforced.

Assume that the previous period (previous day for example), the system has been operating for $t_i > 0$ periods, and the total number of people who migrated from one compartment to the other is m_i. In this case the migration rate would be

$$\alpha_i = \frac{m_i}{t_i} \tag{11}$$

On the other hand, assuming that the following period, new s_i migration cases for the same states have been observed (recorded in the system as proposed in Section 2). This means that the new migration rate would be

$$\alpha_{i+1} = \frac{m_i + s_i}{t_i + 1}. \tag{12}$$

Using Equation 6 to substitute m_i in Equation 13, the new migration rate becomes,

$$\alpha_{i+1} = \frac{t_i \alpha_i + s_i}{t_i + 1}. \tag{13}$$

It is important to mention that,

$$\lim_{t_i \longrightarrow \infty} \alpha_{i+1} = \alpha_i.$$

This shows that keeping on reinforcing the migration rates, gives a more accurate prediction model. This is why the parameters may not be assumed to be constant nor the

Preprints (www.preprints.org) | NOT PEER-REVIEWED | Posted: 29 July 2022 doi:10.20944/preprints202207.0461.v1

may be accurately approximated by some data. This highlights the fact that reinforcing the migration rates implies the reinforcement of the prediction model.

4. Performance evaluation

We use Monte Carlo simulation for experiment. In this section, we explain the setup of the experiment. We consider a region where 4 different plasmodium species are observed (the case of Rwanda for example). According to Proposition 2, the number of possible malaria types, in this case, is, mathematically $n = 2^4 - 1 = 15$. In reality, all possible types may not be observed in a region. This is due to the particularity of a region and the fact that some plasmodium species cannot naturally live together. This is why even if 15 different types of malaria may occur, we consider a case where only 6 of them have been recorded.

The aim, here, is to investigate the effect of periodically reinforcing the proposed model.

Simulation has been done using Python packages (Mathplotlib, Numpy and Random). Here, a numerical solution has been first computed using Euler method [57] run 360 times and the time period considered is $dt = 0.1\ day = 2\ hours\ 24\ minutes = 144\ minutes$.

4.1. Initial conditions

Table 1 represents the numbers of individuals in each compartment, for each malaria type. The letter M stands for Million ($2M$ stands for two millions).

Table 2 shows the initial migration rates considered for each malaria type. Furthermore, we consider a case of a region containing five main medical centres (five sub regions). Subregions are named as *Noth*, *South*, *East*, *Ouest* and *Main City* as it is done to name provinces in many African countries (Rwanda for example). For each subregion, the interval of expected malaria test is shown in Table 3. The table also contains the expected chance of positive test and the probability of suffering each malaria type. A random number of daily (turnout) tests is chosen in the Test interval column, and the probabilities are applied to know the infection status (positive or negative and which malaria type in case the test is positive) of the corresponding individual.

Table 1: Initial compartments and corresponding species.

Compartment/ Species	V_1	V_2	V_3	V_4	V_5	V_6
Susceptible	2M	2M	2M	2M	2M	2M
Protected	2M	2M	2M	2M	2M	2M
Infected	56	60	80	70	30	40
Treated	90	80	20	80	80	50
Recovered	4	86	300	700	800	670

The reason for no variety for Susceptible and Protected, is that, we have assumed that many people may, initially, be susceptible or protected for each malaria type.

Table 2: Initial migration rates.

Rates/ Compartment	V_1	V_2	V_3	V_4	V_5	V_6
a	0.12	0.13	0.2	0.14	0.15	0.16
b	0.21	0.12	0.23	0.11	0.11	0.13
c	0.16	0.17	0.21	0.13	0.14	0.15
d	0.16	0.13	0.21	0.15	0.14	0.12
e	0.14	0.15	0.23	0.11	0.12	0.10
f	0.11	0.15	0.22	0.31	0.51	0.41
u	0.1	0.1	0.1	0.1	0.1	0.31
v	0.1	0.1	0.1	0.72	0.41	0.11
w	0.1	0.19	0.81	0.2	0.1	0.1

Preprints (www.preprints.org) | NOT PEER-REVIEWED | Posted: 29 July 2022 doi:10.20944/preprints202207.0461.v1

Table 3: Parameters configuration.

Medical Center/ quantities	Test	+ chance	V_1	V_2	V_3	V_4	V_5	V_6
Main city	0 - 3	80%	$\frac{1}{10}$	$\frac{2}{10}$	$\frac{3}{10}$	$\frac{1}{10}$	$\frac{2}{10}$	$\frac{1}{10}$
North	0- 50	85%	$\frac{1}{10}$	$\frac{1}{10}$	$\frac{1}{10}$	$\frac{2}{10}$	$\frac{2}{10}$	$\frac{3}{10}$
South	0- 20	90%	$\frac{1}{10}$	$\frac{1}{10}$	$\frac{1}{10}$	$\frac{2}{10}$	$\frac{2}{10}$	$\frac{3}{10}$
Est	0-15	79%	$\frac{2}{10}$	$\frac{2}{10}$	$\frac{2}{10}$	$\frac{2}{10}$	$\frac{1}{10}$	$\frac{1}{10}$
Ouest	0-12	75%	$\frac{1}{10}$	$\frac{2}{10}$	$\frac{1}{10}$	$\frac{2}{10}$	$\frac{1}{10}$	$\frac{3}{10}$

4.2. Effect of constant rates

We first consider the case where all migration rates are constant to visualise the initial predictions, aiming further comparisons.

Preprints (www.preprints.org) | NOT PEER-REVIEWED | Posted: 29 July 2022 doi:10.20944/preprints202207.0461.v1

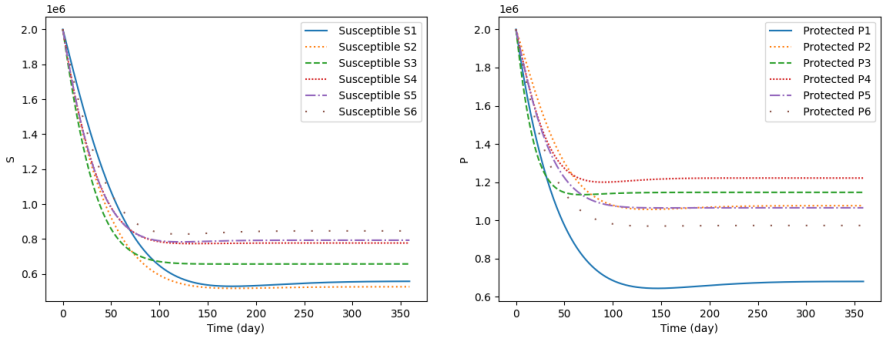

(a) Susceptible. **(b)** Protected.

Figure 4. Susceptible and Protected.

Figures 4a and 4b shows that for all considered malaria types, the number of susceptible, firstly decreases sharply towards a converging point. Figure 4a shows that the susceptibility of malaria of type V_6 converges first and V_2 converges last. On the other hand Figure 4b shows that in terms of susceptibility, the type V_3 converges first and V_1 converges last. The convergence here is influenced by all the compartments and rates and hence can be observed rather than predicted.

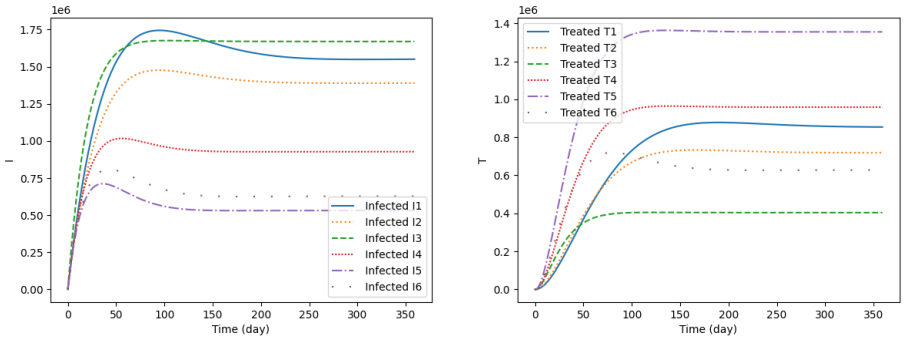

(a) Infected. **(b)** Treated.

Figure 5. Infected and Treated.

Figures 5a and 5b show the trend of the number of infected and treated, respectively. For both figures, some types correspond to an increase and then a convergence but other types show an increase up to the maximum, followed by a short decrease towards a converging point. This highlights the fact that the trends vary from type to type. Hence, the figures show that there is no single trend to describe all malaria types.

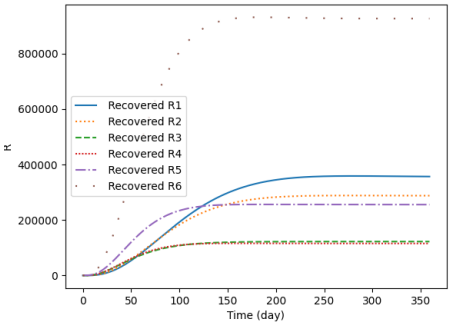

Figure 6. Recovered.

Preprints (www.preprints.org) | NOT PEER-REVIEWED | Posted: 29 July 2022 doi:10.20944/preprints202207.0461.v1

Figure 6 shows the variation of the number of recovered for each malaria type. The figure shows that for all types, there is an increase towards a converging point, though they do not converge at the same time nor at the same point. This confirms the difference in the trends for each type of malaria.

4.3. Effect of reinforced rates

We use the number of new infections to update the migration rate d from susceptible to infected. We explain the practicality of updating the rates based on the system proposed in Section 2. Although the same could be done on the remaining parameters, we have limited to one parameter for two reasons: first, we would trace the effect of updating one parameter on all the compartments, and secondly, we would reduce the number of scenario settings.

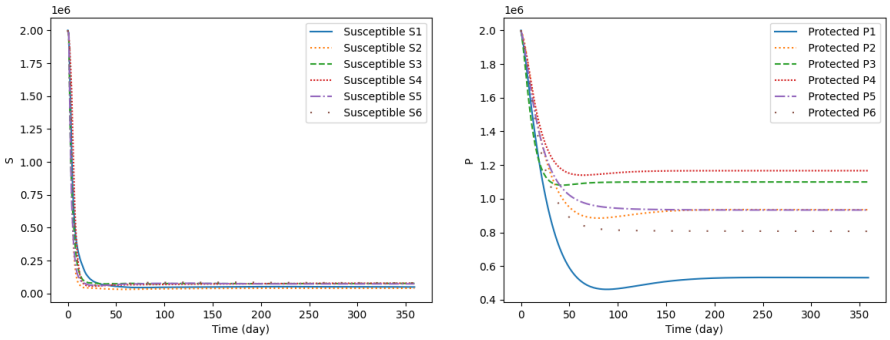

(a) Susceptible. **(b)** Protected.

Figure 7. Susceptible and Protected.

Figure 7a shows that the number of susceptible individuals for each malaria type decreases quicker than in the case Figure 4a, towards the convergence. The figure also shows that for all malaria types, the convergence points are all lesser. On the other hand Figure 7b reveals that the trend shown in Figure 4b has not much changed, though noticeable. However, the convergence points gets lesser for all types of the disease.

Preprints (www.preprints.org) | NOT PEER-REVIEWED | Posted: 29 July 2022 doi:10.20944/preprints202207.0461.v1

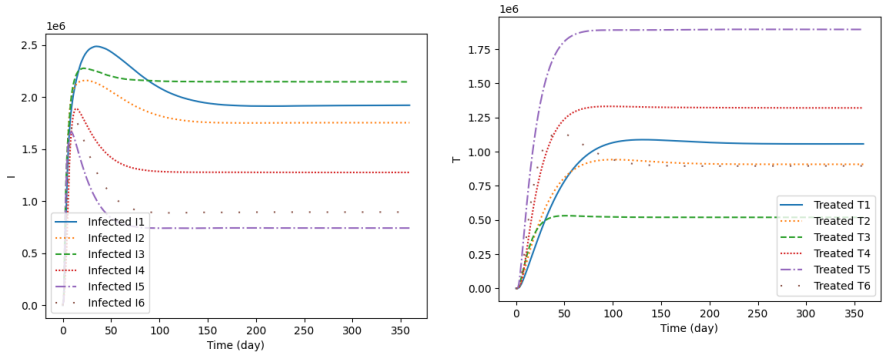

(a) Infected.

(b) Treated.

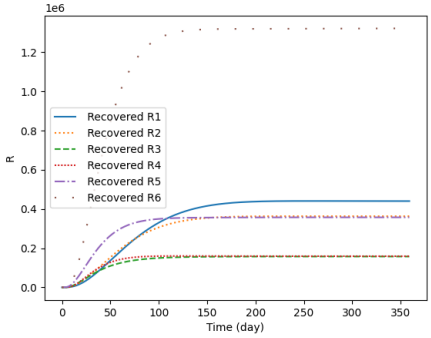

(c) Recovered.

Figure 8. Infected, Treated and Recovered.

Figures 8a, 8b and 8c show that although the trends are almost similar to the case when rates are constants, the convergence points are significantly different.

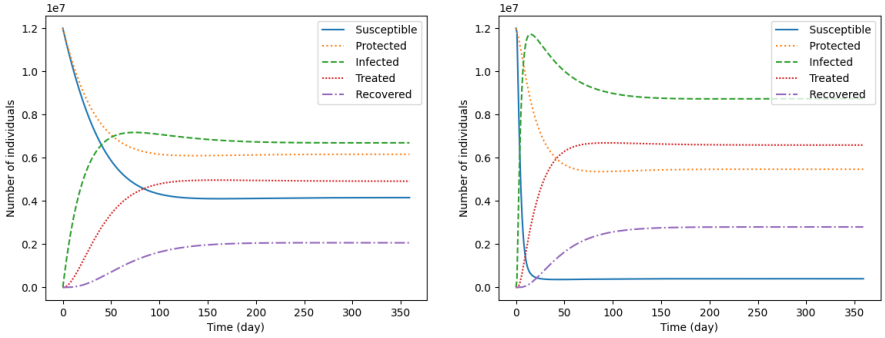

(a) Compartmental variation with constant rates

(b) Compartmental variation with reinforced rates.

Figure 9. Compartmental variation.

Adding all numbers for each compartment, Figures 9a and 9b reveal more clearly the differences. In fact, no curve remains the same, no convergence remains the same, the rates of increase or decrease change and most importantly, the values for each compartment at a given time are significantly different. This highlights the fact that reinforcing the rates provides a significant change in the prediction of the malaria statuses.

4.4. Variation of infectiousness

We use Figure 10 to study the variation of the infectiousness as measured by the parameter d. In fact, Figure 10a shows that, the infectiousness starts by stochastically and

Preprints (www.preprints.org) | NOT PEER-REVIEWED | Posted: 29 July 2022 doi:10.20944/preprints202207.0461.v1

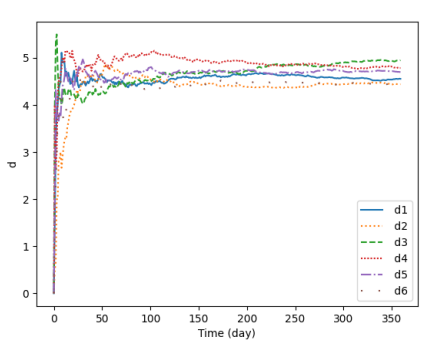

(a) Variation of *d* in terms of *time*.

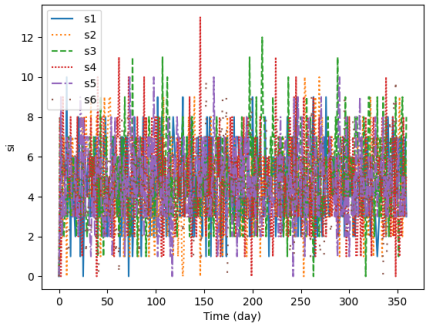

(b) Variation of *si* in terms of *time*.

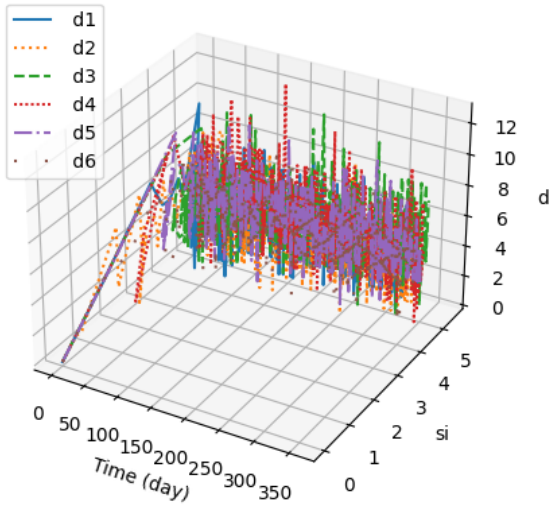

(c) Variation of *d* in terms of *si* and *time*.

Figure 10. Infectiousness variation.

quickly increasing for all malaria variants, until a point where the increase rate significantly decreases. As the time goes, the parameter change decreases for all malaria types. Note that the interdependence and relationship of the different components corresponding to *d* is not noticeable as the corresponding curves cross each other in significantly many occasions. Note that the number of new infections *si* does not show a steady increase or decrease, though stochastic, as shown in Figure 10b. On the other hand, Figure 10c shows that the variation of *d* is shuffled by the randomness of *s*.

5. Conclusion

This paper has provided a dependable digital system model for predicting malaria statuses in the case of mixed infection. The architecture of the data management system has been described and based on it, a predictive model has been proposed. The stability of the system has been studied and the rate reinforcement scheme has been explained and analysed. Results have revealed that there is a significant difference in adopting the rate reinforcements and this emphasises the need for such a digital system for malaria diagnosis. Furthermore, the case of mixed infection may rise some visualisation issues, due to multiple malaria types observable. This also brings up the need for an advanced visualisation system with filtering capabilities.

References

1. Lalremruata, A.; Jeyaraj, S.; Engleitner, T.; Joanny, F.; Lang, A.; Bélard, S.; Mombo-Ngoma, G.; Ramharter, M.; Kremsner, P.G.; Mordmüller, B.; others. Species and genotype diversity of Plasmodium in malaria patients from Gabon analysed by next generation sequencing. *Malaria journal* **2017**, *16*, 1–11.
2. Jagannathan, P.; Kakuru, A. Malaria in 2022: Increasing challenges, cautious optimism. *Nature communications* **2022**, *13*, 1–3.
3. Dahal, P.; Khanal, B.; Rai, K.; Kattel, V.; Yadav, S.; Bhattarai, N.R. Challenges in Laboratory Diagnosis of Malaria in a Low-Resource Country at Tertiary Care in Eastern Nepal: A Comparative Study of Conventional vs. Molecular Methodologies. *Journal of Tropical Medicine* **2021**, *2021*.
4. Okell, L.C.; Ghani, A.C.; Lyons, E.; Drakeley, C.J. Submicroscopic infection in Plasmodium falciparum-endemic populations: a systematic review and meta-analysis. *The Journal of infectious diseases* **2009**, *200*, 1509–1517.
5. Yu, H.; Yang, F.; Rajaraman, S.; Ersoy, I.; Moallem, G.; Poostchi, M.; Palaniappan, K.; Antani, S.; Maude, R.J.; Jaeger, S. Malaria Screener: a smartphone application for automated malaria screening. *BMC Infectious Diseases* **2020**, *20*, 1–8.
6. Kermack, W.; McKendrick, A. Contributions to the mathematical theory of epidemics—I. *Bulletin of Mathematical Biology* **1991**, *53*, 33–55.
7. Tuyishimire, E.; Niyigena, J.d.D.; Tubanambazi, F.M.; Rutikanga, J.U.; Gatabazi, P.; Bagula, A.; Niyigaba, E. A Novel Epidemic Model for the Interference Spread in the Internet of Things. *Information* **2022**, *13*, 181.
8. Tuyishimire, E.; Bagula, B.A. Modelling and analysis of interference diffusion in the internet of things: an epidemic model. 2020 Conference on Information Communications Technology and Society (ICTAS). IEEE, 2020, pp. 1–6.
9. Kuniya, T. Structure of epidemic models: toward further applications in economics. *The Japanese Economic Review* **2021**, *72*, 581–607.
10. Mandal, S.; Sarkar, R.R.; Sinha, S. Mathematical models of malaria-a review. *Malaria journal* **2011**, *10*, 1–19.
11. Aragón, L.E.; Espinal, C. Expansión de la frontera, expansión de la enfermeded: movilidad geográfica y salud en la Amazonia. *Enfoque Integral de la Salud Humana en la Amazonia* **1992**, pp. 429–456.
12. Briët, O.J.; Vounatsou, P.; Gunawardena, D.M.; Galappaththy, G.N.; Amerasinghe, P.H. Models for short term malaria prediction in Sri Lanka. *Malaria Journal* **2008**, *7*, 1–11.
13. Abellana, R.; Ascaso, C.; Aponte, J.; Saute, F.; Nhalungo, D.; Nhacolo, A.; Alonso, P. Spatio-seasonal modeling of the incidence rate of malaria in Mozambique. *Malaria Journal* **2008**, *7*, 1–11.
14. Yé, Y.; Louis, V.R.; Simboro, S.; Sauerborn, R. Effect of meteorological factors on clinical malaria risk among children: an assessment using village-based meteorological stations and community-based parasitological survey. *BMC Public Health* **2007**, *7*, 1–11.
15. Laxminarayan, R. ACT Now or Later: The Economics of Malaria Resistance. Technical report, 2003.
16. Martens, P.; Kovats, R.; Nijhof, S.; De Vries, P.; Livermore, M.; Bradley, D.; Cox, J.; McMichael, A. Climate change and future populations at risk of malaria. *Global environmental change* **1999**, *9*, S89–S107.
17. Amexo, M.; Tolhurst, R.; Barnish, G.; Bates, I. Malaria misdiagnosis: effects on the poor and vulnerable. *The Lancet* **2004**, *364*, 1896–1898.
18. Wyse, A.P.P.; Bevilacqua, L.; Rafikov, M. Simulating malaria model for different treatment intensities in a variable environment. *ecological modelling* **2007**, *206*, 322–330.
19. Sachs, J.; Malaney, P. The economic and social burden of malaria. *Nature* **2002**, *415*, 680–685.
20. Van Lieshout, M.; Kovats, R.; Livermore, M.; Martens, P. Climate change and malaria: analysis of the SRES climate and socio-economic scenarios. *Global environmental change* **2004**, *14*, 87–99.
21. Lindblade, K.A.; Walker, E.D.; Wilson, M.L. Early warning of malaria epidemics in African highlands using Anopheles (Diptera: Culicidae) indoor resting density. *Journal of medical entomology* **2000**, *37*, 664–674.
22. Sandia-Mago, A. Venezuela: malaria y movilidad humana estacional de las comunidades indigenas del rio riecito del estado Apure. *Fermentum* **1994**, *3*, 102–123.
23. Yang, H.M. Malaria transmission model for different levels of acquired immunity and temperature-dependent parameters (vector). *Revista de saude publica* **2000**, *34*, 223–231.
24. Killeen, G.F.; Smith, T.A. Exploring the contributions of bed nets, cattle, insecticides and excitorepellency to malaria control: a deterministic model of mosquito host-seeking behaviour and mortality. *Transactions of the Royal Society of Tropical Medicine and Hygiene* **2007**, *101*, 867–880.
25. Hoshen, M.B.; Morse, A.P. A weather-driven model of malaria transmission. *Malaria journal* **2004**, *3*, 1–14.
26. Yé, Y.; Hoshen, M.; Kyobutungi, C.; Louis, V.R.; Sauerborn, R. Local scale prediction of Plasmodium falciparum malaria transmission in an endemic region using temperature and rainfall. *Global health action* **2009**, *2*, 1923.
27. Parham, P.E.; Michael, E. Modeling the effects of weather and climate change on malaria transmission. *Environmental health perspectives* **2010**, *118*, 620–626.
28. Tuyishimire, E.; Bagula, A.; Rekhis, S.; Boudriga, N. Cooperative Data Muling from Ground Sensors to Base Stations Using UAVs **2017**.

29. Jibreel, F.; Tuyishimire, E.; Daabo, I. An Enhanced Heterogeneous Gateway-Based Energy-Aware Multi-hop Routing Protocol for Wireless Sensor Networks **2022**.
30. Tuyishimire, E.; Bagula, A.; Ismail, A. Clustered data muling in the internet of things in motion. *Sensors* **2019**, *19*, 484.
31. Bagula, A.; Ajayi, O.; Maluleke, H. Cyber physical systems dependability using cps-iot monitoring. *Sensors* **2021**, *21*, 2761.
32. WHO. Malaria surveillance, monitoring & evaluation: a reference manual, 2018.
33. Jensen, M. Making the connection: Africa and the Internet. *Current History* **2000**, *99*, 215.
34. Tuyishimire, E.; Bagula, B.A.; Ismail, A. Optimal clustering for efficient data muling in the internet-of-things in motion. International Symposium on Ubiquitous Networking. Springer, 2018, pp. 359–371.
35. Vishwanath, K.V.; Greenberg, A.; Reed, D.A. Modular data centers: how to design them? Proceedings of the 1st ACM workshop on Large-Scale system and application performance, 2009, pp. 3–10.
36. Sun, H.; Lee, S. Case study of data centers' energy performance. *Energy and Buildings* **2006**, *38*, 522–533.
37. Akintoye, S.B. Quality of service in cloud computing: Data model; resource allocation; and data availability and security **2019**.
38. Abernathey, R.P.; Augspurger, T.; Banihirwe, A.; Blackmon-Luca, C.C.; Crone, T.J.; Gentemann, C.L.; Hamman, J.J.; Henderson, N.; Lepore, C.; McCaie, T.A.; others. Cloud-native repositories for big scientific data. *Computing in Science & Engineering* **2021**, *23*.
39. Güzel, O.; Özdarcan, O. PyWD2015–A new GUI for the Wilson-Devinney code. *Contrib. Astron. Obs. Skalnaté Pleso* **2020**, *50*, 535–538.
40. Oulasvirta, A.; Dayama, N.R.; Shiripour, M.; John, M.; Karrenbauer, A. Combinatorial optimization of graphical user interface designs. *Proceedings of the IEEE* **2020**, *108*, 434–464.
41. Mauwa, H.; Bagula, A.; Tuyishimire, E.; Ngqondi, T. An optimal spectrum allocation strategy for dynamic spectrum markets. 2019 International Conference on Wireless and Mobile Computing, Networking and Communications (WiMob). IEEE, 2019, pp. 1–8.
42. Tuyishimire, E.; Bagula, B.A. A Formal and Efficient Routing Model for Persistent Traffics in the Internet of Things. 2020 Conference on Information Communications Technology and Society (ICTAS). IEEE, 2020, pp. 1–6.
43. Tuyishimire, E.; Bagula, A.; Rekhis, S.; Boudriga, N. Trajectory Planing for Cooperating Unmanned Aerial Vehicles in the IoT. *IoT* **2022**, *3*, 147–168.
44. Tuyishimire, E.; Adiel, I.; Rekhis, S.; Bagula, B.A.; Boudriga, N. Internet of Things in Motion: A Cooperative Data Muling Model Under Revisit Constraints. Ubiquitous Intelligence & Computing, Advanced and Trusted Computing, Scalable Computing and Communications, Cloud and Big Data Computing, Internet of People, and Smart World Congress (UIC/ATC/ScalCom/CBDCom/IoP/SmartWorld), 2016 Intl IEEE Conferences. IEEE, 2016, pp. 1123–1130.
45. Bagula, A.; Tuyishimire, E.; Wadepoel, J.; Boudriga, N.; Rekhis, S. Internet-of-Things in Motion: A Cooperative Data Muling Model for Public Safety. Ubiquitous Intelligence & Computing, Advanced and Trusted Computing, Scalable Computing and Communications, Cloud and Big Data Computing, Internet of People, and Smart World Congress (UIC/ATC/ScalCom/CBDCom/IoP/SmartWorld), 2016 Intl IEEE Conferences. IEEE, 2016, pp. 17–24.
46. Ismail, A.; Bagula, B.A.; Tuyishimire, E. Internet-of-things in motion: A uav coalition model for remote sensing in smart cities. *Sensors* **2018**, *18*, 2184.
47. Ismail, A.; Tuyishimire, E.; Bagula, A. Generating dubins path for fixed wing uavs in search missions. International Symposium on Ubiquitous Networking. Springer, 2018, pp. 347–358.
48. Akintoye, S.B.; Bagula, A.B.; Isafiade, O.E.; Djemaiel, Y.; Boudriga, N. Data model for cloud computing environment. International Conference on e-Infrastructure and e-Services for Developing Countries. Springer, 2018, pp. 199–215.
49. Kassim, Y.M.; Yang, F.; Yu, H.; Maude, R.J.; Jaeger, S. Diagnosing Malaria Patients with Plasmodium falciparum and vivax Using Deep Learning for Thick Smear Images. *Diagnostics* **2021**, *11*, 1994.
50. Kassim, Y.M.; Palaniappan, K.; Yang, F.; Poostchi, M.; Palaniappan, N.; Maude, R.J.; Antani, S.; Jaeger, S. Clustering-based dual deep learning architecture for detecting red blood cells in malaria diagnostic smears. *IEEE Journal of Biomedical and Health Informatics* **2020**, *25*, 1735–1746.
51. Sacharidis, D.; Mukamakuza, C.P.; Werthner, H. Fairness and diversity in social-based recommender systems. Adjunct Publication of the 28th ACM Conference on User Modeling, Adaptation and Personalization, 2020, pp. 83–88.
52. Lin, L.J. *Reinforcement learning for robots using neural networks*; Carnegie Mellon University, 1992.
53. Wang, J.; Zeng, H.; Chen, Z.; Lu, H.; Tao, L.; Ma, W.Y. Recom: reinforcement clustering of multi-type interrelated data objects. Proceedings of the 26th annual international ACM SIGIR conference on Research and development in informaion retrieval, 2003, pp. 274–281.
54. Kobe, F.; Koya, P.R. Controlling the spread of malaria disease using intervention strategies. *interactions* **2015**, *2*.
55. Roberts, M.G.; Heesterbeek, J. Characterizing the next-generation matrix and basic reproduction number in ecological epidemiology. *Journal of mathematical biology* **2013**, *66*, 1045–1064.
56. Szabó, P.; Galanda, J. Sage math for education and research. 2017 15th International Conference on Emerging eLearning Technologies and Applications (ICETA). IEEE, 2017, pp. 1–4.
57. Biswas, B.; Chatterjee, S.; Mukherjee, S.; Pal, S. A discussion on Euler method: A review. *Electronic Journal of Mathematical Analysis and Applications* **2013**, *1*, 2090–2792.